A&A 492, 609–616 (2008)
DOI: 10.1051/0004-6361:200811019

Astronomy
&
Astrophysics

Experimental oscillator strengths and hyperfine constants in Nb II

H. Nilsson and S. Ivarsson

Atomic Astrophysics, Lund Observatory, Box 43, 221 00 Lund, Sweden
e-mail: `[hampus.nilsson;stefan.ivarsson]@astro.lu.se`

Received 23 September 2008 / Accepted 14 October 2008

ABSTRACT

We used high-resolution Fourier transform spectroscopy to measure new and improved transition probabilities and hyperfine data for singly ionized niobium. Intensity calibrated spectra were used to measure branching fractions of 145 Nb II lines in the wavelength interval 2600–4600 Å. Combining the branching fractions with previously reported lifetimes, absolute oscillator strengths for these 145 transitions were derived. In addition, line structures due to magnetic hyperfine interaction were studied resulting in new hyperfine splitting constants for 28 even and 24 odd energy levels.

Key words. atomic data – methods: laboratory – techniques: spectroscopic – line: identification – line: profiles

1. Introduction

Niobium (Nb) is a member of the 4d-transition group known as the palladium group elements, and it has atomic number 41. However, up to the 1950s the official name of this element was columbium (Cb), and it may still be found listed as such in older publications. Niobium has only one naturally occurring isotope (^{93}Nb) with many spectral lines exhibiting the effect of hyperfine structure (hfs) due to the large magnetic moment, $\mu/\mu_N = 6.2$ (Sheriff & Williams 1951), and a large nuclear spin, $I = 9/2$.

Spectral lines of singly ionized niobium, Nb II, are observed in the spectra of many astronomical objects. Niobium plays an important role in the investigation of the chemical evolution of the heavy elements through the s-process (Smith & Wallerstein 1983; Smith & Lambert 1984; Jaschek & Jaschek 1995). A detailed and accurate interpretation of high-resolution stellar spectra requires the inclusion of nuclear effects, such as hyperfine structure and isotopic shifts. Recent publications concerning the abundance of niobium include studies on ultra-metal-poor halo stars (Ivans et al. 2005; Hill et al. 2002; Sneden et al. 2000), abundance investigations of chemically peculiar stars (Yushchenko et al. 2004) and an analysis of early solar system evolution using meteoritic data (Schönbächler et al. 2003). However, it is unclear whether these studies include a detailed hfs model of Nb II, but given the small number of published experimental hfs data for this ion, it is highly unlikely.

The atomic energy level structure of Nb II was extended by Ryabtsev et al. (2000) as part of a project at Lund which aim at improving the atomic data for the singly ionized 4d-transition group. Within this project the term analyses of Y II (Nilsson et al. 1991), Mo II (Nilsson & Pickering 2003), Ru II (Karlsson et al. 2002), Pd II (Litzén et al. 2001) and Ag II (Kalus et al. 2002) have been published, and analyses of Zr II and Rh II are in progress. Oscillator strengths have been measured in Zr II (Sikström et al. 1999; Ljung et al. 2006), Mo II (Sikström et al. 2001), Ru II (Johansson et al. 1994) and Pd II (Lundberg et al. 1996).

The only published laboratory oscillator strengths for Nb II currently available in atomic line databases and used for stellar abundance determinations originate from a paper published by Hannaford et al. (1985), who measured experimental lifetimes with laser induced fluorescence (LIF), and re-scaled intensities from the work by Corliss & Bozman (1962). Experimental hfs for five levels in Nb II have been reported by Young et al. (1995).

This paper presents results based on laboratory spectra recorded with the UV Fourier transform (FT) spectrometer at Lund Observatory. The advantages using this instrument are high spectral resolution, a linear wavenumber scale and a well determined instrumental response function. Intensity calibrated spectra were used to derive branching fractions (BFs) for a total of 145 Nb II transitions. Combining the BFs with the radiative lifetimes reported by Hannaford et al. (1985), we present a large set of absolute oscillator strengths, see Table 4. In addition to the BF measurements we have determined magnetic hfs, $A_{\rm hfs}$-values, for energy levels associated with lines that exhibit broadening due to resolved hfs in our FT spectra.

2. Experiment

The spectra of niobium were recorded with the Lund Chelsea Instruments UV FT spectrometer. A water cooled hollow cathode (HC) discharge lamp was used as light source, with a pure niobium cathode. Recordings were made in the spectral region 20 000–40 000 cm^{-1} (5000–2500 Å), using both neon and argon as carrier gases at a pressure between 0.7 and 1.2 Torr and an instrumental resolution of 0.035 cm^{-1}. In order to check for possible effects of self absorption, the cathode current was varied between 0.2 and 0.7 A, and separate spectra was recorded. Intensity ratios of lines from the same upper level were plotted as a function of the current to verify that the plasma was optically thin for the lines studied. The instrumental response was

Article published by EDP Sciences

Table 1. Hyperfine constants ($A_{\rm hfs}$) in mK ($1K = 1$ cm^{-1}) for even parity levels in Nb II compared with laser measurements and theoretical calculations by Young et al. (1995).

Level	C.G.	$A_{\rm hfs}$ (mK)			
	cm^{-1}	This work[1]	Unc (%)	Y1[1]	Y2[2]
a^5D_0	0.000	0			
a^5D_1	158.984	–8.28	4		
a^5D_2	438.361	–7.30	4		–5.4
a^5D_3	801.326	–6.00	4		
a^5D_4	1224.823	–4.50	4		
a^5F_1	2356.816	–38.20	3		
a^5F_2	2629.132	17.12	2		15.2
a^5F_3	3029.629	29.41	2		
a^5F_4	3542.561	33.02	2		
a^5F_5	4146.037	34.45	2		
a^3P_0	5562.241	0			
a^3P_1	6192.310	2.31	4		
a^3P_2	7261.324	6.80	3		6.5
a^3F_2	7505.765	30.50	2		29.8
a^3F_3	7900.644	6.50	3		
a^3F_4	8320.373	–0.51	5		
a^3H_4	9509.604	14.96	4		
a^3H_5	9812.452	11.55	4		
$4d^4$ a^3H_6	10 186.390	2.92	5		
a^3G_3	10 246.955	1.36	5		
a^3G_4	10 604.229	13.58	4		
a^3G_5	10 918.474	21.61	2		
a^3D_2	12 805.965	25.40	2	25.28[3]	24.3[3]
b^3F_2	13 479.460	35.81	2		29.30[3]
b^3F_3	13 690.228	13.79	2	14.01	
b^3F_4	13 665.686	2.54	4	2.76	
a^3D_3	13 054.696	18.15	4		
a^1G_4	14 790.755	22.12	4		

[1] Experimental values from Young et al. (1995); [2] theoretical values from Young et al. (1995); [3] Young et al. (1995) have used the level designation from Moore (1952), while we have adopted the new label given by Ryabtsev et al. (2000).

determined with internal calibration using known branching ratios (BRs) in Ar II from Whaling et al. (1993).

2.1. Atomic structure of Nb II

As with many other transition elements Nb II has three low metastable configurations, $4d^4$, $4d^3 5s$ and $4d^2 5s^2$, starting at 0,2357 and 20 658 cm^{-1} respectively see Fig. 1. Nb II is the first element in the singly ionized palladium group where $4d^k$ is the ground configuration.

Adding a 5s-electron to the lowest term in Nb III (a ^{4}F) gives rise to two terms; a^5F and a^3F, while adding a 5p-electron yields six terms (z^5G, z^5F, z^5D, z^3G, z^3F and z^3D). Since $4d^4$ only has one quintet term (a^5D), the odd 5p quintets with the parent term ^4F should decay to the two terms $4d^4$ a^5D or $4d^3(^4F)5s$ a^5F in the *LS* coupling scheme. However, the appearance of intercombination lines in Table 3 indicate that *LS* coupling does not provide a complete description of the system.

We have investigated downward transitions from the six lowest odd levels in Nb II with parent term a^4F. Many of these lines are prominent both in laboratory and stellar spectra.

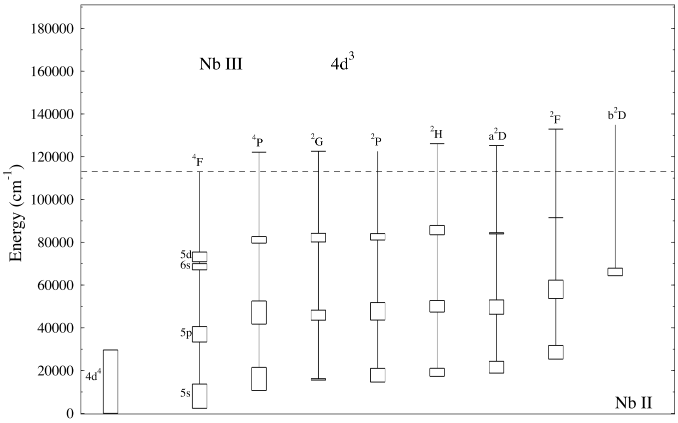

Fig. 1. Partial term diagram of Nb II. Each box represents levels belonging to the same configuration and parent term, except for the $4d^4$ box where the parent term is ambiguous. The parent term designations are from Ryabtsev et al. (2000).

Table 2. Hyperfine constants ($A_{\rm hfs}$) in mK (1 K = 1 cm^{-1}) for odd parity levels in Nb II compared with theoretical calculations by Young et al. (1995).

Level	C.G.	$A_{\rm hfs}$ (mK)		
	cm^{-1}	This work[1]	Unc (%)	(Y1)[1]
z^5G_2	33 351.090	41.00	2	
z^5G_3	33 919.244	20.49	3	
z^5G_4	34 632.033	11.96	3	
z^5G_5	35 474.197	7.57	4	
z^5G_6	36 455.457	3.81	4	
z^3D_1	34 886.354	35.65	2	35.35
z^3D_2	35 553.238	–0.05	4	
z^5F_1	36 520.822	6.80	4	6.80
z^3D_3	36 553.238	–0.05	4	
z^5F_1	36 731.805	40.16	2	
z^5F_2	36 962.774	15.00	3	
z^5F_3	37 376.901	7.35	3	
z^5F_4	37 528.382	4.68	4	
z^5F_5	38 024.336	6.40	4	
z^5D_0	37 298.242	0		
z^5D_1	37 480.076	–4.50	4	
z^5D_2	37 797.316	–4.00	4	
z^5D_3	38 216.387	–3.20	4	
z^5D_4	38 291.252	–0.50	4	
z^3G_3	38 684.960	22.50	2	
z^3G_4	39 335.270	12.29	3	
z^3G_5	40 103.605	7.30	3	
z^3F_2	38 984.387	25.85	2	
z^3F_3	39 779.919	11.49	3	
z^3F_4	40 561.018	5.35	4	

[1] Experimental values from Young et al. (1995).

2.2. Branching fractions

The BF of an emission line from an upper level u to a lower level l is defined as:

$$(BF)_{ul} = A_{ul} / \sum_k A_{uk} = I_{ul} / \sum_k I_{uk}, \qquad (1)$$

where A_{ul} is the transition probability of the line and I_{ul} is the intensity measured in photons per second. A_{uk} and I_{uk} are the

Table 3. Nb II branching fractions (*BF*) and *gf*-values. Lines sorted by upper level.

Upper	Lower	$\lambda_{\rm air}$	σ	*BF*		*A*	*gf*	Unc.	Log(*gf*)
level	level	(Å)	(cm^{-1})	Calc.	Exp.	(s^{-1})		(% in *gf*)	
4d^3(^{4}F)5p z^{5}G$_2$	4d^3(^{4}F)5s a^{5}F$_1$	3225.471	30 994.274	0.750	0.742	1.257E+08	0.981	8	−0.008
τ = 5.9(4)ns	4d^3(^{4}F)5s a^{5}F$_2$	3254.062	30 721.958	0.227	0.234	3.972E+07	0.315	12	−0.501
	4d^3(^{4}F)5s a^{5}F$_3$	3297.045	30 321.461	0.015	0.017	2.856E+06	0.023	32	−1.633
Residual					0.007				
4d^3(^{4}F)5p z^{5}G$_3$	4d^3(^{4}F)5s a^{5}F$_2$	3194.974	31 290.112	0.731	0.713	1.230E+08	1.319	6	+0.120
τ = 5.8(3)ns	4d^3(^{4}F)5s a^{5}F$_3$	3236.400	30 889.615	0.249	0.265	4.568E+07	0.502	11	−0.299
	4d^3(^{4}F)5s a^{5}F$_4$	3291.051	30 376.683	0.013	0.015	2.517E+06	0.029	32	−1.543
Residual					0.007				
4d^3(^{4}F)5p z^{5}G$_4$	d^3(^{4}F)5s a^{5}F$_3$	3163.401	31 602.404	0.774	0.758	1.38E+08	1.862	6	+0.270
τ = 5.5(3)ns	d^3(^{4}F)5s a^{5}F$_4$	3215.594	31 089.472	0.212	0.229	4.17E+07	0.582	13	−0.235
Residual					0.013				
4d^3(^{4}F)5p z^{3}D$_1$	4d^4 a^{5}D$_0$	2865.609	34 886.354	0.108	0.102	1.792E+07	0.066	12	−1.179
τ = 5.7(3)ns	4d^3(^{4}F)5s a^{5}F$_1$	3073.236	32 529.538	0.108	0.087	1.528E+07	0.065	12	−1.188
	4d^3(^{4}F)5s a^{5}F$_2$	3099.181	32 257.222	0.169	0.156	2.741E+07	0.118	8	−0.926
	4d^4 a^{3}P$_0$	3409.185	29 324.113	0.133	0.147	2.580E+07	0.135	9	−0.870
	4d^4 a^{3}P$_1$	3484.046	28 694.044	0.085	0.090	1.579E+07	0.086	9	−1.064
	4d^4 a^{3}F$_2$	3651.182	27 380.589	0.292	0.312	5.482E+07	0.329	9	−0.483
	4d^4 a^{3}D$_2$	4527.636	22 080.389	0.031	0.031	5.522E+06	0.051	13	−1.293
Residual					0.074				
4d^3(^{4}F)5p z^{5}G$_5$	d^3(^{4}F)5s a^{5}F$_4$	3130.783	31 931.636	0.857	0.847	1.599E+08	2.586	6	+0.413
τ = 5.3(3)ns	d^3(^{4}F)5s a^{5}F$_5$	3191.094	31 328.160	0.137	0.147	2.765E+07	0.465	16	−0.333
Residual					0.006				
4d^3(^{4}F)5p z^{3}D$_2$	4d^4 a^{5}D$_1$	2827.075	35 361.838	0.151	0.140	2.448E+07	0.147	9	−0.833
τ = 5.7(3)ns	4d^3(^{4}F)5s a^{5}F$_1$	3014.439	33 164.006	0.028	0.020	3.590E+06	0.024	40	−1.611
	4d^3(^{4}F)5s a^{5}F$_2$	3039.397	32 891.690	0.066	0.045	7.881E+06	0.055	22	−1.263
	4d^3(^{4}F)5s a^{5}F$_3$	3076.863	32491.193	0.230	0.227	3.989E+07	0.283	9	−0.548
	4d^4 a^{3}P$_1$	3408.673	29 328.512	0.153	0.172	3.023E+07	0.263	10	−0.579
	4d^4 a^{3}P$_2$	3537.622	28 259.498	0.066	0.067	1.169E+07	0.110	10	−0.960
	4d^4 a^{3}F$_3$	3619.509	27 620.178	0.208	0.222	3.902E+07	0.383	10	−0.416
	4d^3(^{4}F)5s b^{3}F$_3$	4579.444	21 830.594	0.023	0.034	6.019E+06	0.095	40	−1.024
Residual					0.072				
4d^3(^{4}F)5p z^{5}G$_6$	d^3(^{4}F)5s a^{5}F$_5$	3094.174	32 309.420	1.000	1.000	1.96E+08	3.661	6	+0.564
τ = 5.1(3)ns									
Residual					0.000				
4d^3(^{4}F)5p z^{3}D$_3$	4d^4 a^{5}D$_2$	2768.124	36114.877	0.207	0.197	3.941E+07	0.317	15	−0.499
τ = 5.0(3)ns	4d^4 a^{5}D$_4$	2829.750	35 328.415	0.010	0.017	3.337E+06	0.028	52	−1.552
	4d^3(^{4}F)5s a^{5}F$_2$	2946.895	33 924.106	0.075	0.055	1.101E+07	0.100	25	−0.998
	4d^3(^{4}F)5s a^{5}F$_3$	2982.102	33 523.609	0.124	0.076	1.510E+07	0.141	19	−0.851
	4d^3(^{4}F)5s a^{5}F$_4$	3028.441	33 010.677	0.292	0.325	6.496E+07	0.626	16	−0.204
	4d^4 a^{3}P$_2$	3412.932	29 291.914	0.098	0.130	2.608E+07	0.319	17	−0.496
	4d^4 a^{3}F$_3$	3489.087	28 652.594	0.025	0.033	6.535E+06	0.084	19	−1.078
	4d^4 a^{3}F$_4$	3540.959	28 232.865	0.112	0.141	2.817E+07	0.371	13	−0.431
	4d^4 a^{3}D$_3$	4254.385	23 498.542	0.011	0.015	3.091E+06	0.059	52	−1.231
	4d^3(^{4}F)5s b^{3}F$_4$	4367.960	22 887.552	0.018	0.023	4.671E+06	0.094	20	−1.029
Residual					0.027				
4d^3(^{4}F)5p z^{5}F$_1$	4d^4 a^{5}D$_0$	2721.630	36 731.805	0.039	0.054	1.139E+07	0.038	51	−1.421
τ = 4.7(3)ns	4d^4 a^{5}D$_1$	2733.462	36 572.821	0.087	0.124	2.631E+07	0.088	35	−1.053
	4d^3(^{4}F)5s a^{5}F$_1$	2908.240	34 374.989	0.512	0.487	1.035E+08	0.394	11	
	4d^3(^{4}F)5s a^{5}F$_2$	2931.464	34102.673	0.129	0.145	3.092E+07	0.120	22	−0.922
	4d^4 a^{3}P$_0$	3207.331	31 169.564	0.057	0.043	9.139E+06	0.042	20	−1.374
	4d^4 a^{3}P$_1$	3273.505	30 539.495	0.034	0.027	5.785E+06	0.028	34	−1.554
	4d^4 a^{3}F$_2$	3420.625	29 226.040	0.089	0.068	1.441E+07	0.076	19	−1.120
Residual					0.053				
4d^3(^{4}F)5p z^{5}F$_2$	4d^4 a^{5}D$_1$	2716.306	36 803.790	0.041	0.056	1.191E+07	0.066	50	−1.181
τ = 4.7(3)ns	4d^4 a^{5}D$_2$	2737.085	36 524.413	0.103	0.114	2.429E+07	0.136	31	−0.865
	4d^3(^{4}F)5s a^{5}F$_1$	2888.829	34 605.958	0.187	0.191	4.072E+07	0.255	16	−0.594
	4d^3(^{4}F)5s a^{5}F$_2$	2911.742	34 333.642	0.373	0.391	8.319E+07	0.529	13	−0.277
	4d^3(^{4}F)5s a^{5}F$_3$	2946.110	33 933.145	0.078	*Bl*^{a}				

Table 3. continued.

Upper	Lower	λ_{air}	σ	*BF*		A	gf	Unc.	Log(gf)
level	level	(Å)	(cm^{-1})	Calc.	Exp.	(s^{-1})		(% in gf)	
	4d^4 a^{3}P$_1$	3248.932	30 770.464	0.065	0.047	9.905E+06	0.078	18	−1.106
	4d^4 a^{3}P$_2$	3365.872	29 701.450	0.025	0.016	3.382E+06	0.029	34	−1.542
	4d^4 a^{3}F$_3$	3439.918	29 062.130	0.066	0.048	1.019E+07	0.090	18	−1.044
	4d^4 a^{3}D$_2$	4138.452	24 156.809	0.011	0.008	1.729E+06	0.022	52	−1.654
Residual					0.129				
4d^3(^{4}F)5p z^{5}D$_0$	4d^4 a^{5}D$_1$	2691.770	37 139.258	0.461	0.464	1.497E+08	0.163	20	−0.789
τ = 3.1(3)ns	4d^3(^{4}F)5s a^{5}F$_1$	2861.092	34 941.426	0.527	0.524	1.690E+08	0.208	19	−0.683
Residual					0.012				
4d^3(^{4}F)5p z^{5}F$_3$	4d^4 a^{5}D$_2$	2706.397	36 938.540	0.018	0.034	7.270E+06	0.056	51	−1.252
τ = 4.7(3)ns	4d^4 a^{5}D$_3$	2733.256	36 575.575	0.136	0.151	3.207E+07	0.252	30	−0.599
	4d^3(^{4}F)5s a^{5}F$_2$	2877.038	34 747.769	0.173	0.219	4.653E+07	0.404	15	−0.393
	4d^3(^{4}F)5s a^{5}F$_3$	2910.587	34 347.272	0.349	0.366	7.789E+07	0.693	13	−0.159
	4d^4 a^{3}P$_2$	3319.585	30 115.577	0.082	0.050	1.069E+07	0.124	17	−0.908
	4d^4 a^{3}F$_2$	3346.751	29 871.136	0.033	0.024	5.017E+06	0.059	22	−1.229
	4d^4 a^{3}F$_3$	3391.587	29 476.257	0.012	0.005	1.163E+06	0.014	48	−1.852
	4d^4 a^{3}F$_4$	3440.581	29 056.528	0.112	0.077	1.629E+07	0.202	17	−0.694
	4d^4 a^{3}D$_3$	4110.309	24 322.205	0.012	0.007	1.395E+06	0.025	52	−1.606
	4d^3(^{4}F)5s b^{3}F$_4$	4216.226	23 711.215	0.014	0.009	1.893E+06	0.035	30	−1.452
Residual					0.059				
4d^3(^{4}F)5p z^{5}D$_1$	4d^4 a^{5}D$_0$	2667.291	37 480.076	0.155	0.166	5.363E+07	0.172	28	−0.765
τ = 3.1(3)ns	4d^4 a^{5}D$_1$	2678.654	37321.092	0.040	0.027	8.586E+06	0.028	55	−1.557
	4d^4 a^{5}D$_2$	2698.858	37 041.715	0.256	0.258	8.334E+07	0.273	25	−0.564
	4d^3(^{4}F)5s a^{5}F$_1$	2846.279	35 123.260	0.159	0.159	5.122E+07	0.187	28	−0.729
	4d^3(^{4}F)5s a^{5}F$_2$	2868.521	34 850.944	0.356	*Bl*^{b}	1.148E+08	0.565	50	−0.371
Residual					0.390				
4d^3(^{4}F)5p z^{5}F$_4$	4d^4 a^{5}D$_3$	2721.982	36 727.056	0.222	0.235	5.110E+07	0.511	14	−0.291
τ = 4.6(3)ns	4d^3(^{4}F)5s a^{5}F$_3$	2897.806	34 498.753	0.179	0.171	3.727E+07	0.423	16	−0.374
	4d^3(^{4}F)5s a^{5}F$_4$	2941.543	33 985.821	0.411	0.355	7.709E+07	0.901	14	−0.045
	4d^3(^{4}F)5s a^{5}F$_5$	2994.722	33 382.345	0.148	0.195	4.249E+07	0.515	16	−0.289
	4d^4 a^{3}F$_3$	3374.246	29 627.738	0.016	0.019	4.221E+06	0.065	19	−1.188
Residual					0.024				
4d^3(^{4}F)5p z^{5}D$_2$	4d^4 a^{5}D$_1$	2656.075	37 638.332	0.156	0.148	4.617E+07	0.244	32	−0.612
τ = 3.2(3)ns	4d^4 a^{5}D$_2$	2675.939	37 358.955	0.116	0.112	3.489E+07	0.187	38	−0.727
	4d^4 a^{5}D$_3$	2702.194	36 995.990	0.169	0.182	5.676E+07	0.311	28	−0.507
	4d^3(^{4}F)5s a^{5}F$_2$	2842.643	35 168.184	0.136	0.136	4.248E+07	0.257	28	−0.589
	4d^3(^{4}F)5s a^{5}F$_3$	2875.390	34 767.687	0.349	0.348	1.089E+08	0.675	21	−0.171
	4d^4 a^{3}P$_1$	3163.140	31 605.006	0.020	0.018	5.530E+06	0.042	49	−1.382
	4d^4 a^{3}P$_2$	3273.880	30 535.992	0.008	0.008	2.617E+06	0.021	53	−1.677
	4d^4 a^{3}F$_3$	3343.892	29 896.672	0.016	0.019	5.815E+06	0.049	41	−1.312
Residual					0.030				
4d^3(^{4}F)5p z^{5}F$_5$	4d^4 a^{5}D$_4$	2716.622	36 799.513	0.223	0.220	4.777E+07	0.582	18	−0.235
τ = 4.6(3)ns	4d^3(^{4}F)5s a^{5}F$_4$	2899.233	34 481.775	0.135	0.150	3.267E+07	0.453	21	−0.344
	4d^3(^{4}F)5s a^{5}F$_5$	2950.880	33 878.299	0.573	0.549	1.194E+08	1.716	12	+0.235
	4d^4 a^{3}F$_4$	3365.587	29 703.963	0.037	0.045	9.800E+06	0.183	20	−0.737
	4d^4 a^{3}H$_6$	3591.194	27 837.946	0.008	0.011	2.287E+06	0.049	36	−1.313
	4d^4 a^{3}G$_5$	3688.189	27 105.862	0.008	0.007	1.609E+06	0.036	44	−1.442
	4d^3(^{4}F)5s b^{3}F$_4$	4104.160	24 358.650	0.008	0.010	2.079E+06	0.058	36	−1.238
Residual					0.008				
4d^3(^{4}F)5p z^{5}D$_3$	4d^4 a^{5}D$_2$	2646.253	37 778.026	0.121	0.130	3.815E+07	0.281	28	−0.552
τ = 3.4(3)ns	4d^4 a^{5}D$_3$	2671.926	37 415.061	0.213	0.210	6.182E+07	0.463	21	−0.334
	4d^4 a^{5}D$_4$	2702.517	36 991.564	0.080	0.078	2.306E+07	0.177	33	−0.752
	4d^3(^{4}F)5s a^{5}F$_3$	2841.143	35 186.758	0.090	0.083	2.433E+07	0.206	26	−0.686
	4d^3(^{4}F)5s a^{5}F$_4$	2883.174	34 673.826	0.362	0.359	1.056E+08	0.922	15	−0.035
	4d^4 a^{3}P$_2$	3229.557	30 955.063	0.050	0.055	1.611E+07	0.176	20	−0.753
	4d^4 a^{3}F$_4$	3343.966	29 896.014	0.036	0.037	1.089E+07	0.128	22	−0.893
Residual					0.048				
4d^3(^{4}F)5p z^{5}D$_4$	4d^4 a^{5}D$_3$	2666.590	37489.926	0.057	0.056	1.696E+07	0.163	36	−0.788
τ = 3.3(3)ns	4d^4 a^{5}D$_4$	2697.059	37 066.429	0.402	0.388	1.176E+08	1.155	17	+0.062

Table 3. continued.

Upper	Lower	$\lambda_{\rm air}$	σ	*BF*		*A*	*gf*	Unc.	Log(*gf*)
level	level	(Å)	(cm^{-1})	Calc.	Exp.	(s^{-1})		(% in *gf*)	
	4d^3(^{4}F)5s a^{5}F$_4$	2876.962	34 748.691	0.091	*Bl*[a]				
	4d^3(^{4}F)5s a^{5}F$_5$	2927.811	34 145.215	0.396	0.414	1.255E+08	1.453	19	+0.162
	4d^3(^{4}F)5s b^{3}F$_4$	4059.674	24 625.566	0.013	0.010	2.940E+06	0.065	37	−1.184
Residual					0.132				
4d^3(^{4}F)5p z^{3}G$_3$	4d^4 a^{3}P$_2$	3181.398	31 423.636	0.051	0.036	7.114E+06	0.076	22	−1.121
τ = 5.0(3)ns	4d^4 a^{3}F$_2$	3206.340	31 179.195	0.505	0.506	1.012E+08	1.092	8	+0.038
	4d^4 a^{3}F$_3$	3247.470	30 784.316	0.080	0.083	1.661E+07	0.184	11	−0.735
	4d^4 a^{3}H$_4$	3426.568	29 175.356	0.108	0.127	2.541E+07	0.313	10	−0.504
	4d^4 a^{3}G$_3$	3515.416	28 438.005	0.099	0.098	1.961E+07	0.255	10	−0.594
	4d^4 a^{3}D$_2$	3863.042	25 878.995	0.056	0.045	9.061E+06	0.142	11	−0.848
	4d^3(^{2}G)5s b^{3}G$_3$	4321.481	23 133.708	0.012	0.016	3.203E+06	0.063	41	−1.202
Residual					0.089				
4d^3(^{4}F)5p z^{3}F$_2$	4d^4 a^{3}F$_3$	3216.187	31 083.743	0.028	0.029	3.926E+06	0.030	35	−1.516
τ = 7.3(3)ns	4d^4 a^{3}G$_3$	3478.786	28 737.432	0.103	0.117	1.604E+07	0.146	10	−0.837
	4d^4 a^{1}D$_2$	3741.288	26 721.166	0.022	0.028	3.859E+06	0.041	26	−1.392
	4d^4 a^{3}D$_2$	3818.856	26 178.422	0.464	0.399	5.463E+07	0.598	9	−0.224
	4d^4 a^{3}D$_3$	3855.489	25 929.691	0.046	0.044	6.070E+06	0.068	39	−1.170
	4d^4 a^{3}D$_1$	3865.004	25 865.859	0.069	0.096	1.315E+07	0.147	37	−0.832
	4d^3(^{4}F)5s b^{3}F$_2$	3919.701	25 504.927	0.063	0.074	1.012E+07	0.117	11	−0.933
	4d^3(^{4}F)5s b^{3}F$_3$	3952.363	25 294.159	0.065	0.073	1.002E+07	0.117	10	−0.931
Residual					0.140				
4d^3(^{4}F)5p z^{3}G$_4$	4d^3(^{4}F)5s a^{5}F$_4$	2793.041	35 792.709	0.064	0.094	1.843E+07	0.194	46	−0.712
τ = 5.1(3)ns	4d^4 a^{3}F$_3$	3180.285	31 434.626	0.489	0.465	9.127E+07	1.246	9	+0.096
	4d^4 a^{3}F$_4$	3223.326	31 014.897	0.070	0.067	1.307E+07	0.183	15	−0.737
	4d^4 a^{3}H$_5$	3386.238	29 522.818	0.103	0.115	2.265E+07	0.351	11	−0.455
	4d^4 a^{3}G$_3$	3436.821	29 088.315	0.018	0.016	3.182E+06	0.051	36	−1.295
	4d^4 a^{3}G$_4$	3479.560	28 731.041	0.118	0.109	2.133E+07	0.349	12	−0.458
	4d^4 a^{3}D$_3$	3804.012	26 280.574	0.031	0.027	5.332E+06	0.104	16	−0.982
	4d^3(^{4}F)5s b^{3}F$_3$	3898.285	25 645.042	0.051	0.051	1.005E+07	0.206	12	−0.686
	4d^4 a^{1}G$_4$	4073.080	24 544.515	0.011	0.010	1.947E+06	0.044	32	−1.361
Residual					0.045				
4d^3(^{4}F)5p z^{3}F$_3$	4d^4 a^{3}P$_2$	3074.270	32 518.595	0.009	0.014	2.037E+06	0.020	50	−1.694
τ = 6.8(3)ns	4d^4 a^{3}F$_3$	3135.925	31 879.275	0.025	0.032	4.632E+06	0.048	35	−1.320
	4d^4 a^{3}F$_4$	3177.766	31 459.546	0.009	0.010	1.481E+06	0.016	50	−1.804
	4d^4 a^{3}H$_4$	3302.616	30 270.315	0.016	0.019	2.839E+06	0.033	40	−1.488
	4d^4 a^{3}G$_4$	3426.528	29 175.690	0.082	0.092	1.358E+07	0.167	9	−0.776
	4d^4 a^{1}D$_2$	3633.121	27 516.698	0.012	0.014	2.125E+06	0.029	31	−1.531
	4d^4 a^{3}D$_3$	3740.720	26 725.223	0.270	0.228	3.359E+07	0.494	9	−0.307
	4d^3(^{4}F)5s b^{3}F$_2$	3801.136	26 300.459	0.102	0.101	1.481E+07	0.225	9	−0.648
	4d^3(^{4}F)5s b^{3}F$_4$	3828.243	26 114.233	0.063	0.061	8.961E+06	0.138	9	−0.860
	4d^3(^{4}F)5s b^{3}F$_3$	3831.844	26 089.691	0.235	0.249	3.666E+07	0.565	9	−0.248
	4d^4 a^{1}G$_4$	4000.603	24 989.164	0.035	0.038	5.540E+06	0.093	14	−1.031
	4d^3(^{2}G)5s b^{3}G$_3$	4126.178	24 228.667	0.013	0.012	1.829E+06	0.033	31	−1.486
Residual					0.129				
4d^3(^{4}F)5p z^{3}G$_5$	4d^3(^{4}F)5s a^{5}F$_5$	2780.235	35 957.568	0.127	0.163	3.132E+07	0.399	27	−0.399
τ = 5.2(3)ns	4d^4 a^{3}F$_4$	3145.402	31 783.232	0.446	0.417	8.010E+07	1.308	10	+0.117
	4d^4 a^{3}H$_4$	3267.673	309 594.001	0.012	0.012	2.361E+06	0.042	42	−1.381
	4d^4 a^{3}H$_6$	3341.596	29 917.215	0.087	0.098	1.886E+07	0.347	13	−0.459
	4d^4 a^{3}G$_4$	3388.929	29 499.376	0.013	0.014	2.613E+06	0.050	32	−1.305
	4d^4 a^{3}G$_5$	3425.420	29 185.131	0.158	0.149	2.861E+07	0.554	13	−0.257
	4d^3(^{4}F)5s b^{3}F$_4$	3781.372	26 437.919	0.084	0.074	1.428E+07	0.337	13	−0.473
	4d^4 a^{1}G$_4$	3949.445	25 312.850	0.014	0.018	3.422E+06	0.088	28	−1.055
	4d^3(^{2}G)5s b^{3}G$_5$	4156.671	24 050.933	0.016	0.014	2.670E+06	0.076	32	−1.118
Residual					0.042				

[a] Blended line included in the residual; [b] blended line; the theoretical BF is used to derive the log(gf).

corresponding quantities for other transitions from the same upper level. The intensities of the spectral lines were measured as the area under the line profile. In order to get absolute intensities, the recorded intensities were corrected for the instrumental response, which was determined from known argon BRs from Whaling et al. (1993).

Intensities for lines too weak to be measured or outside the recorded wavenumber region are given as a residual which is estimated from theoretical calculations using the Cowan code (Cowan 1981). The good agreement between the experimental and theoretical BFs justifies the use of the calculated residuals. The residuals span from less than 1% to as much as 14%. The

Table 4. Nb II log gf-values. The lines are sorted by wavelength.

λ_{Air}	σ	log gf	
(Å)	(cm^{-1})	This work	Hannaford[a]
2646.253	37 778.026	−0.552	−0.480
2656.075	37 638.332	−0.612	−0.600
2666.590	37 489.926	−0.788	−0.960
2667.291	37 480.076	−0.765	−1.020
2671.926	37 415.061	−0.334	−0.370
2675.939	37 358.955	−0.727	−0.780
2678.654	37 321.092	−1.557	−1.240
2691.770	37 139.258	−0.789	−0.860
2697.059	37 066.429	+0.062	+0.000
2698.858	37 041.715	−0.564	−0.550
2702.194	36 995.990	−0.507	−0.560
2702.517	36 991.564	−0.752	−0.790
2706.397	36 938.540	−1.252	−1.140
2716.306	36 803.790	−1.181	−1.250
2716.622	36 799.513	−0.235	−0.280
2721.630	36 731.805	−1.421	−1.500
2721.982	36 727.056	−0.291	−0.370
2733.256	36 575.575	−0.599	−0.610
2733.462	36 572.821	−1.053	−1.190
2737.085	36 524.413	−0.865	−0.990
2768.124	36 114.877	−0.499	−0.600
2780.235	35 957.568	−0.399	−0.260
2793.041	35 792.709	−0.712	−0.650
2827.075	35 361.838	−0.833	−0.820
2829.750	35 328.415	−1.552	−1.350
2841.143	35 186.758	−0.686	−0.490
2842.643	35 168.184	−0.589	−0.550
2846.279	35 123.260	−0.729	−0.780
2861.092	34 941.426	−0.683	−0.600
2865.609	34 886.354	−1.179	−1.220
2868.521	34 850.944	−0.371[b]	−0.280
2875.390	34 767.687	−0.171	−0.080
2877.038	34 747.769	−0.393	−0.300
2883.174	34 673.826	−0.035	−0.120
2888.829	34 605.958	−0.594	−0.510
2897.806	34 498.753	−0.374	−0.290
2899.233	34 481.775	−0.344	−0.270
2908.240	34 374.989	−0.404	−0.340
2910.587	34 347.272	−0.159	−0.190
2911.742	34 333.642	−0.277	−0.270
2927.811	34 145.215	+0.162	+0.160
2931.464	34 102.673	−0.922	−0.970
2941.543	33 985.821	−0.045	+0.000
2946.895	33 924.106	−0.998	−0.870
2950.880	33 878.299	+0.235	+0.210
2982.102	33 523.609	−0.851	−0.580
2994.722	33 382.345	−0.289	−0.250
3014.439	33 164.006	−1.611	
3028.441	33 010.677	−0.204	−0.410
3039.397	32 891.690	−1.263	−1.570
3073.236	32 529.538	−1.188	−1.220
3074.270	32 518.595	−1.694	
3076.863	32 491.193	−0.548	−0.470
3094.174	32 309.420	+0.564	+0.550
3099.181	32 257.222	−0.926	−1.060
3130.783	31 931.636	+0.413	+0.410
3135.925	31 879.275	−1.320	
3145.402	31 783.232	+0.117	−0.040
3163.140	31 605.006	−1.382	
3163.401	31 602.404	+0.270	+0.260
3177.766	31 459.546	−1.804	
3180.285	31 434.626	+0.096	−0.050
3181.398	31 423.636	−1.121	−0.790
3191.094	31 328.160	−0.333	−0.260
3194.974	31 290.112	+0.120	+0.090
3206.340	31 179.195	+0.038	−0.130
3207.331	31 169.564	−1.374	
3215.594	31 089.472	−0.235	−0.190
3216.187	31 083.743	−1.516	
3223.326	31 014.897	−0.737	−0.740
3225.471	30 994.274	−0.008	−0.030
3229.557	30 955.063	−0.753	−0.670
3236.400	30 889.615	−0.299	−0.290
3247.470	30 784.316	−0.735	−0.280
3248.932	30 770.464	−1.106	−0.830
3254.062	30 721.958	−0.501	−0.420
3267.673	30 594.001	−1.381	
3273.505	30 539.495	−1.554	
3273.880	30 535.992	−1.677	
3291.051	30 376.683	−1.543	−0.950
3297.045	30 321.461	−1.633	
3302.616	30 270.315	−1.488	
3319.585	30 115.577	−0.908	−0.870
3341.596	29 917.215	−0.459	−0.450
3343.892	29 896.672	−1.312	
3343.966	29 896.014	−0.893	−0.850
3346.751	29 871.136	−1.229	
3365.587	29 703.963	−0.737	−0.670
3365.872	29 701.450	−1.542	
3374.246	29 627.738	−1.188	−1.240
3386.238	29 522.818	−0.455	−0.330
3388.929	29 499.376	−1.305	
3391.587	29 476.257	−1.852	
3408.673	29 328.512	−0.579	−0.570
3409.185	29 324.113	−0.870	−0.820
3412.932	29 291.914	−0.496	−0.430
3420.625	29 226.040	−1.120	−0.940
3425.420	29 185.131	−0.257	−0.140
3426.528	29 175.690	−0.776	−0.420
3426.568	29 175.356	−0.504	
3436.821	29 088.315	−1.295	
3439.918	29 062.130	−1.044	−0.860
3440.581	29 056.528	−0.694	−0.630
3478.786	28 737.432	−0.837	
3479.560	28 731.041	−0.458	−0.220
3484.046	28 694.044	−1.064	−1.060
3489.087	28 652.594	−1.078	−0.900
3515.416	28 438.005	−0.594	−0.180
3537.622	28 259.498	−0.960	
3540.959	28 232.865	−0.431	−0.360
3591.194	27 837.946	−1.313	
3619.509	27 620.178	−0.416	−0.380
3633.121	27 516.698	−1.531	
3651.182	27 380.589	−0.483	−0.400
3688.189	27 105.862	−1.442	−0.780
3740.720	26 725.223	−0.307	−0.270
3741.288	26 721.166	−1.392	
3781.372	26 437.919	−0.473	−0.420
3801.136	26 300.459	−0.648	
3804.012	26 280.574	−0.982	
3818.856	26 178.422	−0.224	−0.140
3828.243	26 114.233	−0.860	−1.180
3831.844	26 089.691	−0.248	−0.470
3855.489	25 929.691	−1.170	
3863.042	25 878.995	−0.848	
3865.004	25 865.859	−0.832	
3898.285	25 645.042	−0.686	−0.410
3919.701	25 504.927	−0.933	
3949.445	25 312.850	−1.055	
3952.363	25 294.159	−0.931	−0.590
4000.603	24 989.164	−1.031	−1.070
4059.674	24 625.566	−1.184	
4073.080	24 544.515	−1.361	
4104.160	24 358.650	−1.238	
4110.309	24 322.205	−1.606	
4126.178	24 228.667	−1.486	
4138.452	24 156.809	−1.654	
4156.671	24 050.933	−1.118	−0.800
4216.226	23 711.215	−1.452	
4254.385	23 498.542	−1.231	
4321.481	23 133.708	−1.202	
4367.960	22 887.552	−1.029	−0.960
4527.636	22 080.389	−1.293	−1.400
4579.444	21 830.594	−1.024	−1.240

[a] Hannaford et al. (1985); [b] blended line; the theoretical BF is used to derive the log(gf).

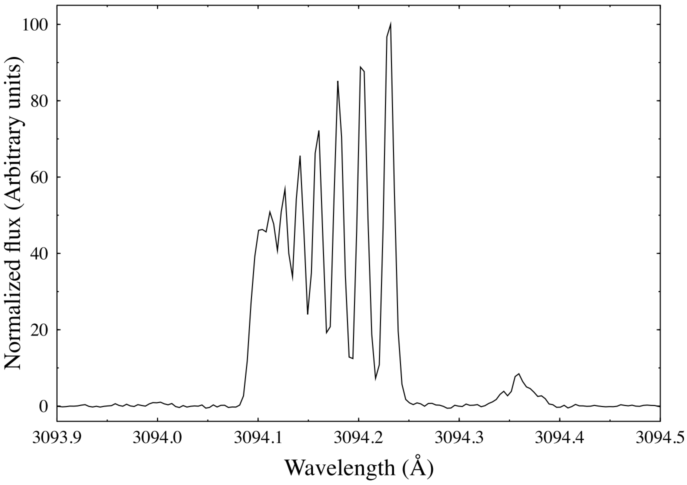

Fig. 2. The structure of the $4d^3(^4F)5s\ a^5F_5$–$4d^3(^4F)5p\ z\ ^5G_6$ transition in Nb II at 3094.17 Å. The large width (almost 0.2 Å) is due to the splitting in the $4d^3(^4F)5s\ a\ ^5F_5$ energy level ($A_{\rm hfs} = 34.45 \times 10^{-3}$ cm^{-1}).

levels, z^5F_2, z^5D_1 and z^5D_4, have a large residuals because of problem with line blending. The theoretical BFs are presented for comparison in column five of Table 3.

2.3. Hyperfine structure

Niobium has a nuclear spin of $I = 9/2$, and as a result many of the Nb II lines investigated show line profiles broadened by hfs, as seen in Fig. 2. We have measured magnetic hyperfine constants ($A_{\rm hfs}$-values) for many of the levels included in the BF measurements it is an important to include hfs in element abundances of high-resolution stellar spectra (Booth & Blackwell 1983). The $A_{\rm hfs}$-value is proportional to the energy level shift according to:

$$\Delta E = 1/2 A_{\rm hfs} C + B_{\rm hfs} f(F, I, J) \qquad (2)$$

where

$$C = F(F+1) - I(I+1) - J(J+1) \qquad (3)$$

and the second term is the electric quadrupole contribution (see e.g. Cowan 1981). No effects of quadrupole interaction were observed in the lines investigated.

The hfs splittings in the line profiles were investigated by fitting a theoretical line structure to the recorded spectral feature using a least-squares fit routine. The fitted parameters were: the $A_{\rm hfs}$-value, the wavenumber position of the components, the relative intensity for the strongest hyperfine component, the line width and the damping factor, where the latter is 1 for a pure Lorentzian profile and 0 for a pure Gaussian profile. Values between 0 and 1 are represented by a Voigt profile. The relative intensity distribution of the individual components is calculated assuming pure IJ coupling. The derived values are reported in Tables 1 and 2. The $A_{\rm hfs}$-values are generally larger for the 5s than for the 4d levels because of the larger penetration of the s-electrons into the atomic core.

We used a statistical approach to estimate the uncertainties of the derived $A_{\rm hfs}$-values. A hyperfine profile based upon the derived values was superimposed with white noise of same SNR as the observed spectral feature, and the standard deviation from a high number of computer fits was taken as the uncertainty associated with the transition investigated.

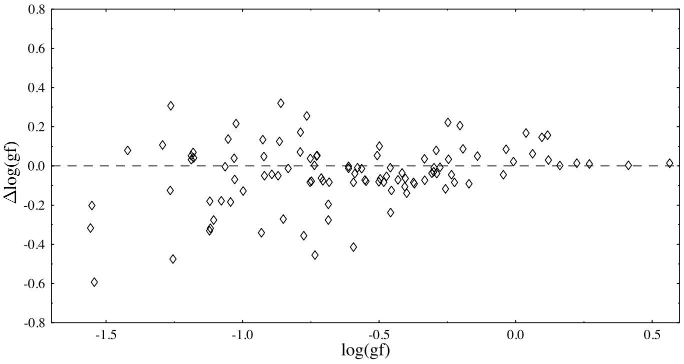

Fig. 3. Comparison between $\log(gf)$-values from our work and the work of Hannaford et al. (1985). $\Delta\log(gf) = \log(gf)_{\rm this\ work} - \log(gf)_{\rm Hannaford}$ is plotted as a function of line strength.

3. Oscillator strengths

Transition probabilities are derived from the BFs and the lifetime τ using Eq. (1) and

$$\tau_u = 1/\sum_k A_{uk}. \qquad (4)$$

The results in Table 3 are sorted by upper level. Figure 3 shows a comparison between our $\log(gf)$-values and the values reported by Hannaford et al. (1985). The uncertainties given in Table 3 are derived using the technique described in Sikström et al. (2002). The uncertainty used for the residual is 50%.

The strongest transition from the $4d^3(^4F)5p\ z^5D_1$ level is blended, but we have chosen to include this level, using the theoretical BF for the blended line. The uncertainty of the blended line is included in the residual and has a large effect on the other lines in this group. It should be noted that the uncertainty used for the residual is 50%.

4. Results

We have measured accurate BFs for 145 lines, using the emission technique. Combining the BFs with lifetimes reported by Hannaford et al. (1985) we have determined 145 absolute oscillator strengths. In Fig. 3 our new $\log(gf)$ values are compared with the values reported by Hannaford et al. (1985). Hyperfine $A_{\rm hfs}$-values have been derived for 52 levels and the $A_{\rm hfs}$-values are compared with experimental and theoretical values from Young et al. (1995). The wavelengths reported in Table 3 are Ritz wavelengths derived from the energy levels reported by Ryabtsev et al. (2000).

Acknowledgements. H.N. acknowledge the financial support from the Lund Laser Centre (LLC) through the Linneaus grant from the Swedish Research Council. We gratefully acknowledge Professor S. Johansson and Dr R. Blackwell-Whitehead for reading the manuscript and Professor U. Litzén for enlightening discussions.

References

Booth, A. J., & Blackwell, D. E. 1983, MNRAS, 204, 777
Corliss, C. H., & Bozman, W. R. 1962, NBS Monograph, 53
Cowan, R. D. 1981, The Theory of Atomic Structure and Spectra (Berkley, CA: University of California)
Hannaford, P., Lowe, R. M., Biemont, E., & Grevesse, N. 1985, A&A, 143, 447
Hill, V., Plez, B., Cayrel, R., et al. 2002, A&A, 387, 560
Ivans, I. I., Sneden, C., Gallino, R., Cowan, J. J., & Preston, G. W. 2005, ApJ, 627, L145

Jaschek, C., & Jaschek, M. 1995, in The Behavior of Chemical Elements in Stars (Cambridge, UK: Cambridge University Press), 338
Johansson, S. G., Joueizadeh, A., Litzen, U., et al. 1994, ApJ, 421, 809
Kalus, G., Litzén, U., Launay, F., & Tchang-Brillet, L. 2002, Phys. Scr, 65, 46
Karlsson, H., Joueizadeh, A., & Johansson, S. 2002, Phys. Scr, 66, 238
Litzén, U., Lundberg, H., Tchang-Brillet, W.-Ü. L., Launay, F., & Engleman, R. J. 2001, Phys. Scr, 64, 63
Ljung, G., Nilsson, H., Asplund, M., & Johansson, S. 2006, A&A, 456, 1181
Lundberg, H., Johansson, S. G., Larsson, J., et al. 1996, ApJ, 469, 388
Moore, C. E. 1952, Atomic Energy Levels, Natl. Bur. Stand. (US) Circ. 467, II
Nilsson, A. E., Johansson, S., & Kurucz, R. L. 1991, Phys. Scr, 44, 226
Nilsson, H., & Pickering, J. C. 2003, Phys. Scr, 67, 223
Ryabtsev, A. N., Churilov, S. S., & Litzén, U. 2000, Phys. Scr, 62, 368
Schönbächler, M., Lee, D.-C., Rehkämper, M., et al. 2003, Earth Planet. Sci. Lett., 216, 467
Sheriff, R. E., & Williams, D. 1951, Phys. Rev., 82, 651
Sikström, C. M., Lundberg, H., Wahlgren, G. M., et al. 1999, A&A, 343, 297
Sikström, C. M., Pihlemark, H., Nilsson, H., et al. 2001, J. Phys. B, Atom. Mol. Phys., 34, 477
Sikström, C. M., Nilsson, H., Litzén, U., Blom, A., & Lundberg, H. 2002, J. Quant. Spec. Radiat. Transf., 74, 355
Smith, V. V., & Lambert, D. L. 1984, PASP, 96, 226
Smith, V. V., & Wallerstein, G. 1983, ApJ, 273, 742
Sneden, C., Cowan, J. J., Ivans, I. I., et al. 2000, ApJ, 533, L139
Whaling, W., Carle, M. T., & Pitt, M. L. 1993, J. Quant. Spec. Radiat. Transf., 50, 7
Young, L., Hasegawa, S., Kurtz, C., Datta, D., & Beck, D. R. 1995, Phys. Rev. A, 51, 3534
Yushchenko, A. V., Gopka, V. F., Kim, C., et al. 2004, A&A, 413, 1105